External Measurement of Small Strain Quasi-elastic Deformation Properties of Toyoura Sand with Torsional Shear and Triaxial Apparatus

by

J. Koseki [1], T. Ono [2] and T. Sato [3], K. Hayano [3] and M. Torimitsu [4]

ABSTRACT

Drained torsional shear and triaxial tests were performed on a hollow cylindrical specimen of Toyoura sand, which was consolidated isotropically after preparation by air-pluviation. Under several stress states, quasi-elastic deformation properties were measured with external displacement transducers by applying very small amplitude cyclic torsional and vertical loads. Under triaxial extension conditions of $\sigma_v' < \sigma_h'$, the shear modulus that was defined on vertical and horizontal planes was found to be basically a function of $(\sigma_v' \sigma_h')^{1/2}$, where σ_v' and σ_h' are the vertical and horizontal stresses, respectively. The results could also be explained by an existing cross-anisotropic hypo-quasi-elastic model, considering inherent and stress state-induced anisotropy in modeling of vertical and horizontal Young's moduli and Poisson's ratios. On the other hand, under triaxial compression conditions of $\sigma_v' > \sigma_h'$, degradation in the externally measured shear modulus and vertical Young's modulus was observed, while its extent was reduced by applying sustained shear stress on the vertical and horizontal planes. Such peculiar behaviors under triaxial compression conditions was estimated to be affected by non-uniform distribution of vertical and torsional shear stresses applied to the specimen.

INTRODUCTION

The shear modulus G_{vh} that was defined on the horizontal plane is one of the essential stress-strain properties of soils in analyzing their seismic responses. The G_{vh} values at small strain levels have been modeled as a function of stress states in a variety of forms (e.g., Jamiolkowski et al., 1995; Tatsuoka and Kohata, 1995), including:

$$G_{vh}/f(e) = G_{vh0}/f(e_0)(\sigma_v'/\sigma_0)^{n_v}(\sigma_h'/\sigma_0)^{n_h} \quad (1)$$

$$G_{vh}/f(e) = G_{vh0}/f(e_0)\{(\sigma_v'+\sigma_h')/(2\sigma_0)\}^{n} \quad (2)$$

$$G_{vh}/f(e) = G_{vh0}/f(e_0)\{(\sigma_v'+2\sigma_h')/(3\sigma_0)\}^{n} \quad (3)$$

---

[1] Junichi Koseki, Associate Professor, Institute of Industrial Science, University of Tokyo

[2] Tatsuya Ono, Graduate Student, Hosei University

[3] Takeshi Sato and Kimitoshi Hayano, Research Associate, IIS, Univ. of Tokyo

[4] Michie Torimitsu, Technical Staff, ditto

where, σ_v' and σ_h' are effective vertical (axial) and horizontal (radial) stresses, respectively; f(e) is a function of the current void ratio e to account for the change in the density during testing, set typically as $f(e)=(2.17-e)^2/(1+e)$ referring to Hardin and Richart (1963); G_{vh0} is a value of G_{vh} under a reference isotropic stress state of $\sigma_v'=\sigma_h'=\sigma_0$ at a reference void ratio of e_0; and n_v, n_h and n are parameters representing the dependency of G_{vh} values on the stress levels. Since it is generally assumed that $n_v=n_h$ (Jamiolkowski et al., 1995), Eq. 1 can be modified with replacing them by $n/2$ as:

$$G_{vh}/f(e) = G_{vh0}/f(e_0)\{(\sigma_v'\sigma_h')^{1/2}/\sigma_0\}^n \quad (4)$$

Recently, Tatsuoka et al. (1999) proposed a different type of formulation based on cross-anisotropic hypo-quasi-elastic modeling, as could be summarized into:

$$G_{vh} = E_v/\{2(1+\nu_0)\}\cdot\{2(1-\nu_0)/(1+aR^n-2a^{1/2}R^{n/2}\nu_0)\} \quad (5)$$

where, E_v is the vertical Young's modulus; R is the stress ratio defined as $R=\sigma_v'/\sigma_h'$; a is a parameter representing the degree of inherent anisotoropy defined as a ratio of vertical and horizontal Young's moduli under isotropic stress states (i.e., $a=E_v/E_h$ at $\sigma_v'=\sigma_h'$); ν_0 is a Poisson's ratio for the isotropic behavior (i.e., $\nu_0=\nu_{vh}=\nu_{hv}$ at $R=a^{-1/n}$, when the horizontal Young's modulus E_h becomes equal to E_v). When the vertical Young's modulus is modeled with Eq.6, referring to Hardin and Bladford (1989) and Tatsuoka and Kohata (1995) among others, Eq.5 can be rewritten as Eq. 7.

$$E_v/f(e) = E_{v0}/f(e_0)(\sigma_v'/\sigma_0)^n \quad (6)$$

$$G_{vh}/f(e) = E_{v0}/f(e_0)/\{2(1+\nu_0)\}\cdot\{(\sigma_v'\sigma_h')^{1/2}/\sigma_0\}^n\cdot\{2(1-\nu_0)/(R^{-n/2}+aR^{n/2}-2a^{1/2}\nu_0)\} \quad (7)$$

where, E_{v0} is is a value of E_v under a reference isotropic stress state of $\sigma_v'=\sigma_h'=\sigma_0$ at a reference void ratio of e_0.

When it is assumed that $G_{vh0}=E_{v0}/\{2(1+\nu_0)\}$, Eq. 4 can be rewritten in a similar manner as:

$$G_{vh}/f(e) = E_{v0}/f(e_0)/\{2(1+\nu_0)\}\cdot\{(\sigma_v'\sigma_h')^{1/2}/\sigma_0\}^n \quad (8)$$

Eq. 7 is different from Eq. 8 by a factor of $\{2(1-\nu_0)/(R^{-n/2}+aR^{n/2}-2a^{1/2}\nu_0)\}$, as appears in the last term of Eq. 7. When the inherent anisotropy is ignored (i.e., a=1.0), this factor becomes unity under isotropic stress state (i.e., R=1.0).

The above modelings suggest that the σ_v' and σ_h' values affect the G_{vh} values in a combied manner. Attempts have been made by several reseachers to compare the experimental data with the above modelings, while number of studies on effects of different anisotropic stress states on the shear modulus are limited (e.g., Yamashita and Suzuki, 1999, among others).

In the present study, therefore, drained torsional shear and triaxial tests were performed on hollow cylindrical specimens of dense Toyoura sand to investigate the effects of different anisotropic stress states on the quasi-elastic shear modulus, as well as those on the quasi-elastic vertical Young's modulus. These quasi-elastic deformation properties were measured externally by applying cyclic torsional and vertical loads with a strain amplitude of about 10^{-5}, under several stress states in the course of isotropic consolidation and triaxial shearing.

APPARATUS AND TESTING PROCEDURES

The torsional shear and triaxial testing apparatus that was employed in the present study is schematically shown in Fig.1. In order to improve the accuracy in controling small amplitude cyclic torsional loads under anisotropic stress states, a modificaiton was made from the one employed by Koseki et al. (2000) with respect to the torsional loading device. Refer to Koseki et al. (2000) for the detailed explanations on the control of apparatus and measurement of data.

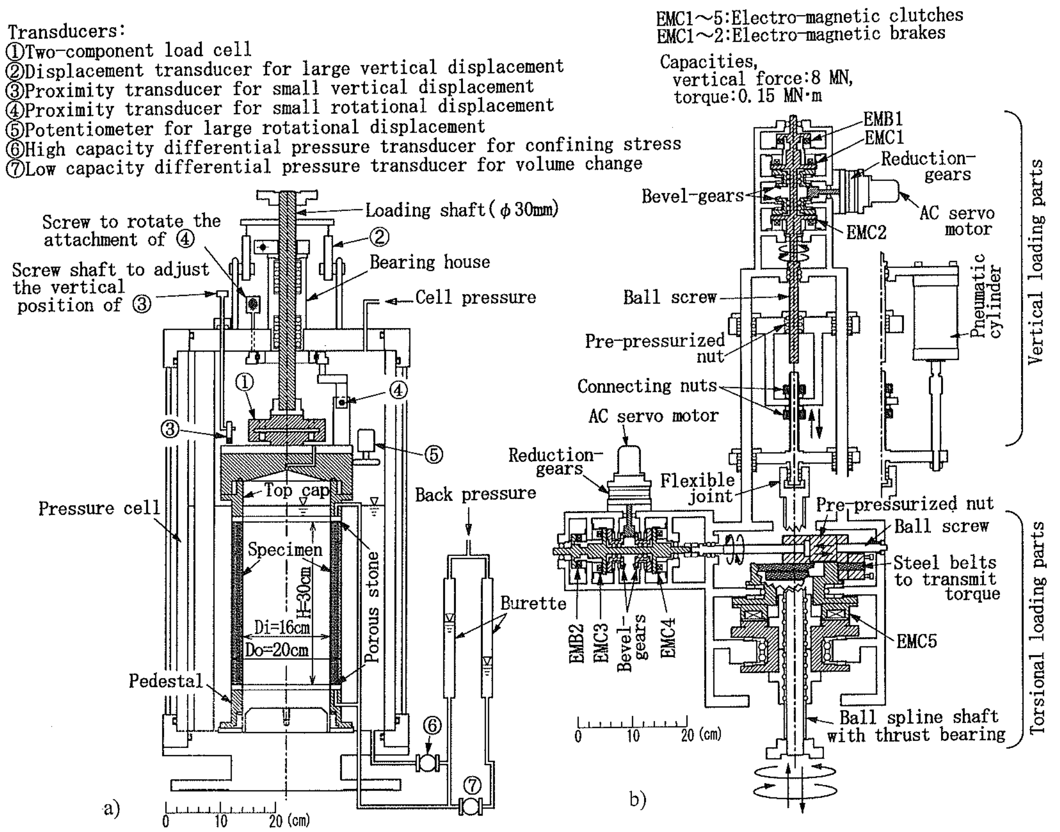

Figure 1. Torsional shear and triaxial testing apparatus; a) pressure cell and specimen, and b) torsional and vertical loading device

A hollow cylindrical specimen with an outer diameter of 20 cm, inner diameter of 16 cm and a height of 30 cm was prepared by pluviating air dried Toyoura sand (e_{max}=0.975, e_{min}=0.561) through air. Under the initial confining stress of 30 kPa, it had a relative density of 60% and was saturated by a combination of vacuuming, flushing with de-aired water, and back-pressurizing (refer to Ampadu and Tatsuoka, 1993, for detailed procedures). It was isotropically consolidated up to confining stress of σ_v'=σ_h'=400 kPa, followed by reduction and restoration in the confining stress to 50 kPa and 100 kPa, respectively (Fig. 2a). Note that the inner and the outer cell pressures were kept equal to each other throughout the tests so that the circumferential stress was always equal to the radial stress.

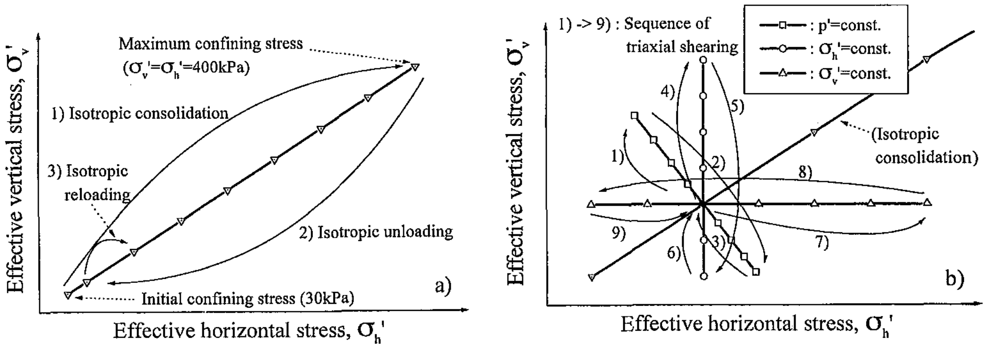

Figure 2. Schematic stress paths employed in a) isotropic consolidation and b) large cyclic shearing

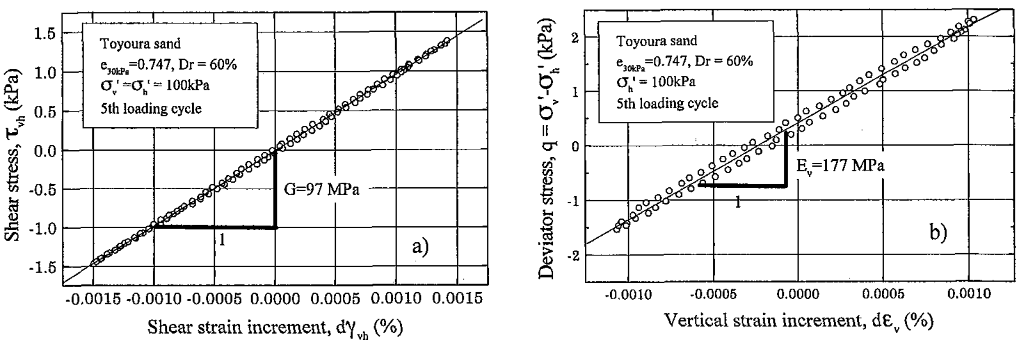

Figure 3. Typical results measured during isotropic consolidation with applying drained small cyclic loadings in a) torsional and b) vertical directions

During isotropic consolidation, after some aging about 10 minutes at several stress levels, six cycles of torsional and vertical loads were applied independently on the specimen, under both drained and undrained conditions with a single amplitude of about 0.0015 % and 0.0010 % for the shear strain increment $d\gamma_{vh}$ and the vertical strain increment $d\varepsilon_v$, respectively. Such small strain increments were evaluated externally by measuring rotational and vertical displacement of the top cap with small-capacity proximity transducers (Fig. 1a). Typical results measured during the fifth loading cycle under drained condition are shown in Fig. 3. Since the measured stress-strain relationships were almost linear, the drained quasi-elastic shear modulus G_{vh} and the drained quasi-elastic vertical Young's modulus E_v were evaluated rather confidently as shown in the figures. The undrained moduli were evaluated in a similar manner based on the results measured under undrained condition, which are not reported in the present paper.

From isotropic stress state at $\sigma_v'=\sigma_h'=100$ kPa, the σ_v' value was increased until the value of the stress ratio R ($=\sigma_v'/\sigma_h'$) became 2, while keeping the effective mean principal stress $p'=(\sigma_v'+2\sigma_h')/3$ constant at 100 kPa (i.e., with decreasing the σ_h' value at $d\sigma_h'=-1/2d\sigma_v'$). While keeping the same p', the σ_v' value was decreased until the R value became 1/2, and then it was restored to 100 kPa. After this first large cyclic shearing, the second large cyclic shearing was conducted by deviating the σ_v' value, while keeping σ_h' constant at 100 kPa. It was followed by the third large cyclic shearing by deviating the σ_h' value while keeping σ_v' constant at 100 kPa. Figure 2b illustrates the stress paths employed in these large cyclic sharing stages.

After the above set of three large cyclic shearing stages that started from the isotropic stress state at $\sigma_v'=\sigma_h'=100$ kPa, similar sets of three large cyclic shearing was conducted from the isotropic stress states at $\sigma_v'=\sigma_h'=200$ kPa and 300 kPa. The final set of large cyclic shearing was conducted after applying a sustained shear stress τ_{vh} of 50 kPa at $\sigma_v'=\sigma_h'=200$ kPa.

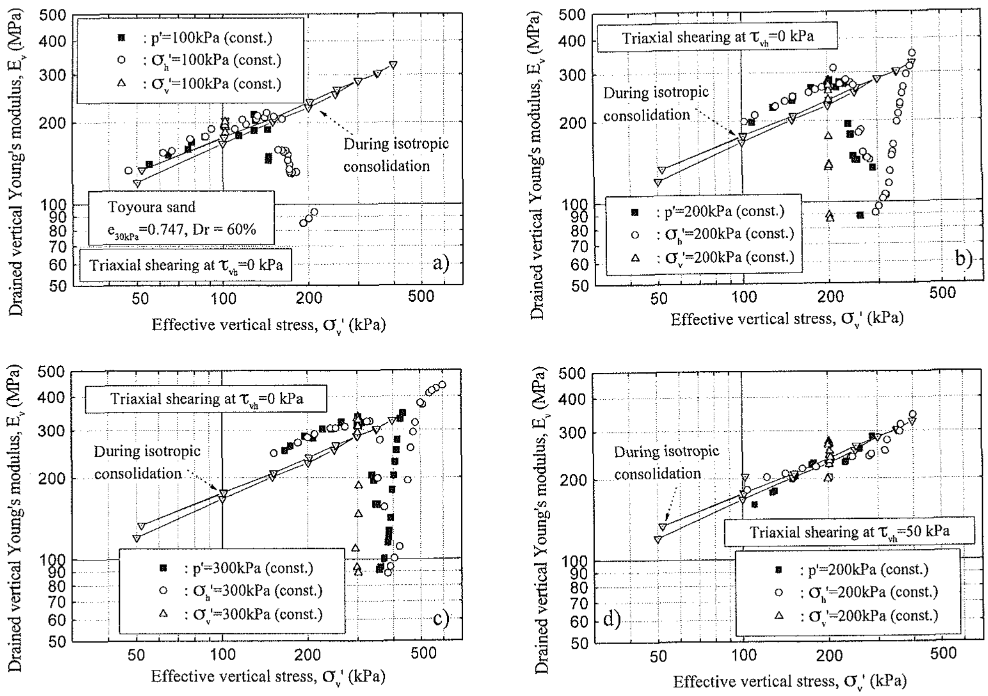

Figure 4. Drained quasi-elastic vertical Young's modulus versus effective vertical stress during triaxial shearing starting from stress states with $\tau_{vh}=0$ at a) $\sigma_v'=\sigma_h'=100$ kPa, b) $\sigma_v'=\sigma_h'=200$ kPa, c) $\sigma_v'=\sigma_h'=300$ kPa, and d) with $\tau_{vh}=50$ kPa at $\sigma_v'=\sigma_h'=200$ kPa

Since it took nearly one month to complete all the sets of large cyclic shearing, it was possible that some of the cell water penetrated the membrane into the specimen, as reported by Tatsuoka et al. (1988). Therefore, the volume change of specimen during triaxial shearing could not be obtained reliably from the volume change of water in a burrete that was connected to the specimen. Conseqently, without correcting for the effects of change in the density of specimen, the measured values of quasi-elasitc moduli were compared to each other in the followings.

RESULTS AND DISCUSSIONS

Drained quasi-elastic vertical Young's modulus

The values of E_v that were measured during isotropic consolidation and triaxial shearing are plotted in Fig. 4 versus the respective σ_v' value where each E_v value was evaluated. When the σ_v' values were smaller than the level of the isotropic effective stress from which the shearing started (i.e., when the σ_v' values were smaller than 100, 200, 300 and 200 kPa in Figs. 4a through 4d, respectively), the relationships between E_v and σ_v' that were measured during shearing were similar to those measured during isotropic consolidation. It is likely that a slight overall increase in the E_v values during shearing compared to those during the isotropic consolidation, as seen from Figs. 4b and 4c, may be due to densification of the specimen that

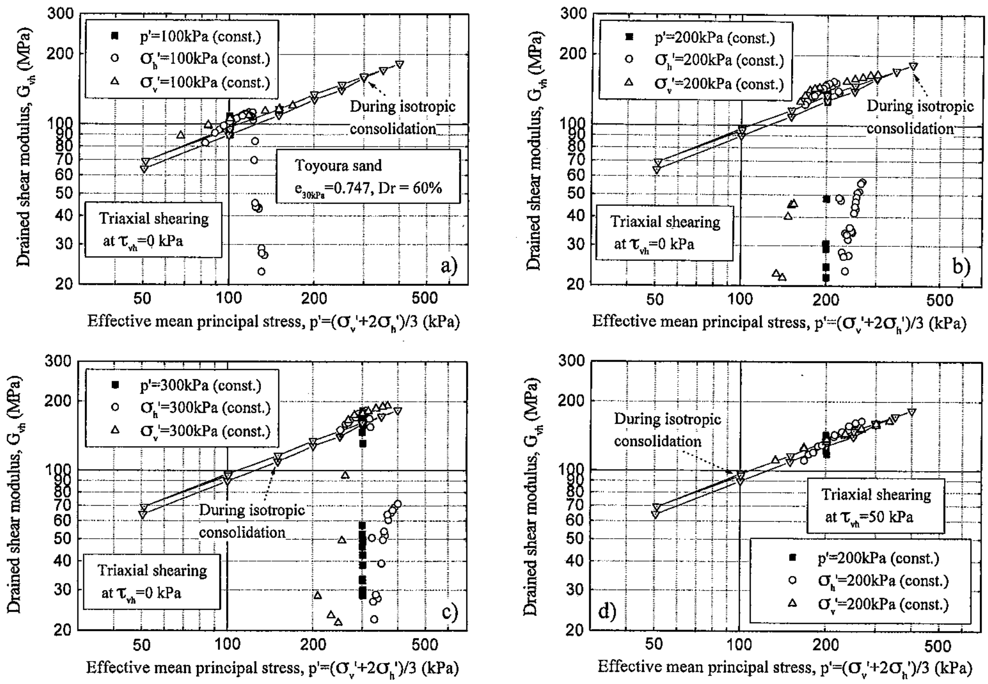

Figure 5. Drained quasi-elastic shear modulus versus effective mean principal stress p' during triaxial shearing starting from stress states with τ_{vh}=0 at a) σ_v'=σ_h'=100 kPa, b) σ_v'=σ_h'=200 kPa, c) σ_v'=σ_h'=300 kPa, and d) with τ_{vh}=50 kPa at σ_v'=σ_h'=200 kPa

occurred during previous large cyclic shearing stages.

On the other hand, when the σ_v' value was increased from the level of the isotropic effective stress from which the shearing started, or when the σ_h' value was decreased while keeping σ_v' constant (i.e., under triaxial compression condition with σ_v'>σ_h'), significant degradation in the E_v values was observed, as shown in Figs. 4a through 4c. In Figs. 4b and 4c, a recovery of the E_v values with the increase in σ_v' was also observed. The extent of degradation in the E_v values was not pronounced in Fig. 4d, which were measured at a sustained shear stress of τ_{vh}=50 kPa.

Interestingly, under the stress states at τ_{vh}=0 (Figs. 4a through 4c), degradation in the E_v values started when the deviator stress q=σ_v'-σ_h'exceeded about 50 kPa. Irrespective of the current stress level of σ_v' or σ_h', the E_v values became minimal when the q value was about 100 kPa, and they started to recover when the q value was further increased. On the other hand, under the stress states with τ_{vh}=50 kPa, no clear correlation could be found between E_v and q (Fig. 4d). Reasons for these peculiar behaviors under triaxial compression conditions are not known to the authors, but they may have been affected by non-uniform distribution of vertical and torsional shear stresses that were applied from the loading device to the specimen through the top cap.

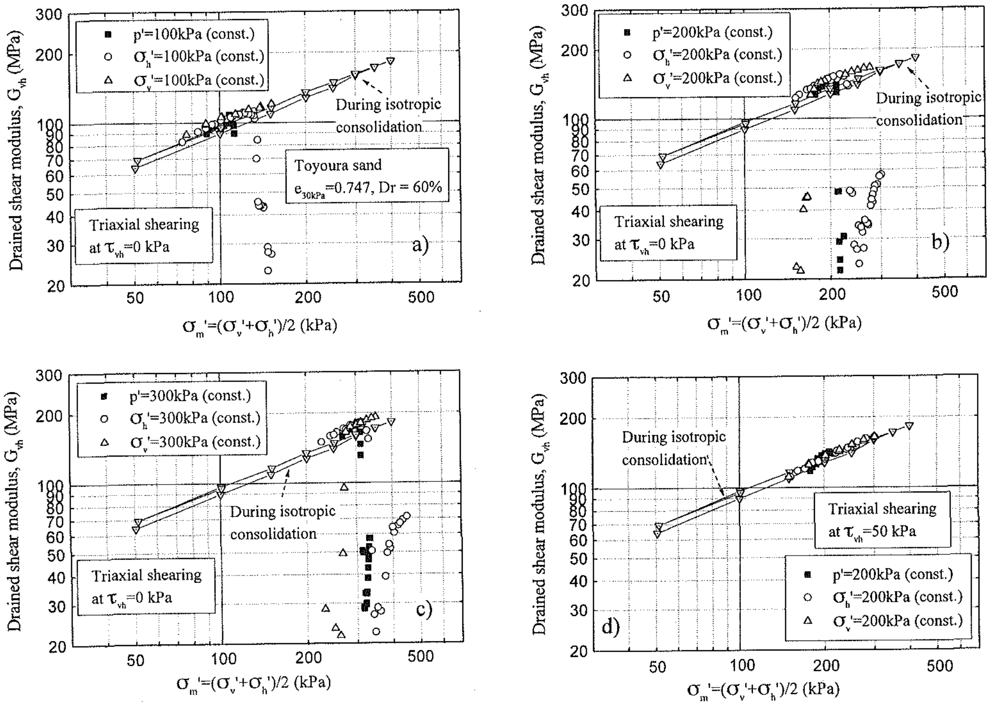

Figure 6. Drained quasi-elastic shear modulus versus σ_m'=(σ_v'+σ_h')/2 during triaxial shearing starting from stress states with τ_{vh}=0 at a) σ_v'=σ_h'=100 kPa, b) σ_v'=σ_h'=200 kPa, c) σ_v'=σ_h'=300 kPa, and d) with τ_{vh}=50 kPa at σ_v'=σ_h'=200 kPa

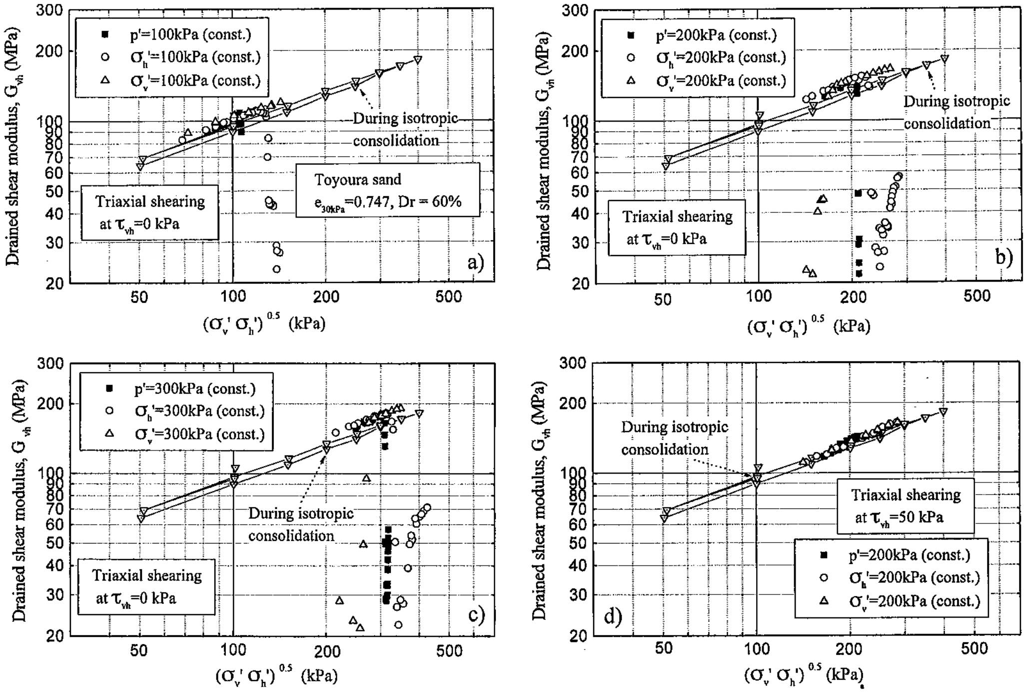

Figure 7. Drained quasi-elastic shear modulus versus $(\sigma_v'\sigma_h')^{1/2}$ during triaxial shearing starting from stress states with $\tau_{vh}=0$ at a) $\sigma_v'=\sigma_h'=100$ kPa, b) $\sigma_v'=\sigma_h'=200$ kPa, c) $\sigma_v'=\sigma_h'=300$ kPa, and d) with $\tau_{vh}=50$ kPa at $\sigma_v'=\sigma_h'=200$ kPa

Drained quasi-elastic shear modulus

Values of G_{vh} that were measured during isotropic consolidation and triaxial shearing are plotted versus the values of $p'=(\sigma_v'+2\sigma_h')/3$, $\sigma_m'=(\sigma_v'+\sigma_h')/2$ and $(\sigma_v'\sigma_h')^{1/2}$ in Figs. 5 through 7, respectively. During triaxial compression, degradation in the G_{vh} values was observed under the stress states with $\tau_{vh}=0$, whereas it was not clearly observed with $\tau_{vh}=50$ kPa. With $\tau_{vh}=0$, the G_{vh} value became minimal when the q value was about 100 kPa, followed by its recovery with further increase in q. These behaviors were qualitatively the same as observed on the E_v values.

On the other hand, except for the region of the extensive degradation, the G_{vh} values measured during triaxial shearing were in general consistent with those measured during isotropic consolidation under the same effective stress levels in terms of p', σ_m' or $(\sigma_v'\sigma_h')^{1/2}$. In addition, it is seen from Figs. 6d, 7d and 8d that, when following the stress path with keeping p' constant at $\tau_{vh}=50$ kPa, the G_{vh} values were not constant but changed according to the subsequent change in the σ_m' or $(\sigma_v'\sigma_h')^{1/2}$ values. Similar behaviors were also observed in other figures with $\tau_{vh}=0$ kPa, when the region of the extensive degradation was excluded. Therefore, the G_{vh} values could be regarded as basically a function of $(\sigma_v'+\sigma_h')/2$ or $(\sigma_v'\sigma_h')^{0.5}$, rather than $p'=(\sigma_v'+2\sigma_h')/3$. Consequently, superiority of Eqs. 2 and 4 over Eq. 3 in modelling the quasi-elastic shear modulus could be obtained from the present test results.

Comparison between measured and predicted quasi-elastic shear moduli

Measured values of G_{vh} are compared with those predicted based on the measured values of E_v using Eqs. 7 and 8 in Figs. 8 and 9, respectively. In the prediction, values of E_{v0} and n were set equal to 177 MPa and 0.44, respectively, based on the E_v values measured during isotropic consolidation as shown in Fig. 4. Note that, in the present study, E_{v0} was defined under a reference stress state of σ_0=100 kPa at a reference void ratio of e_0=0.747 which is equal to the initial void ratio of the specimen under a confining stress of 30 kPa. Values of a and ν_0 were set to 1.1 and 0.15, respectively, based on the test results by Hoque and Tatsuoka (1998).

Except for the region of the extensive degradation, the measured G_{vh} values were larger by about 50 % than those predicted using Eqs. 7 and 8, while the general tendency could be reasonably simulated by these formulations. Reasons for the quantitative discrepancy between measured and predicted G_{vh} values are not known to the authors, but they may be due to the possible effect of end restraint at the both ends of the specimen.

It can be also seen from Figs. 8 and 9 that, under the test conditions employed in the present study (i.e., under the stress ratio $R=\sigma_v'/\sigma_h'$ ranging between 1/2 and 2), the difference between the G_{vh} values predicted using Eqs. 7 and 8 was not noticeable. This is because the ratio of the

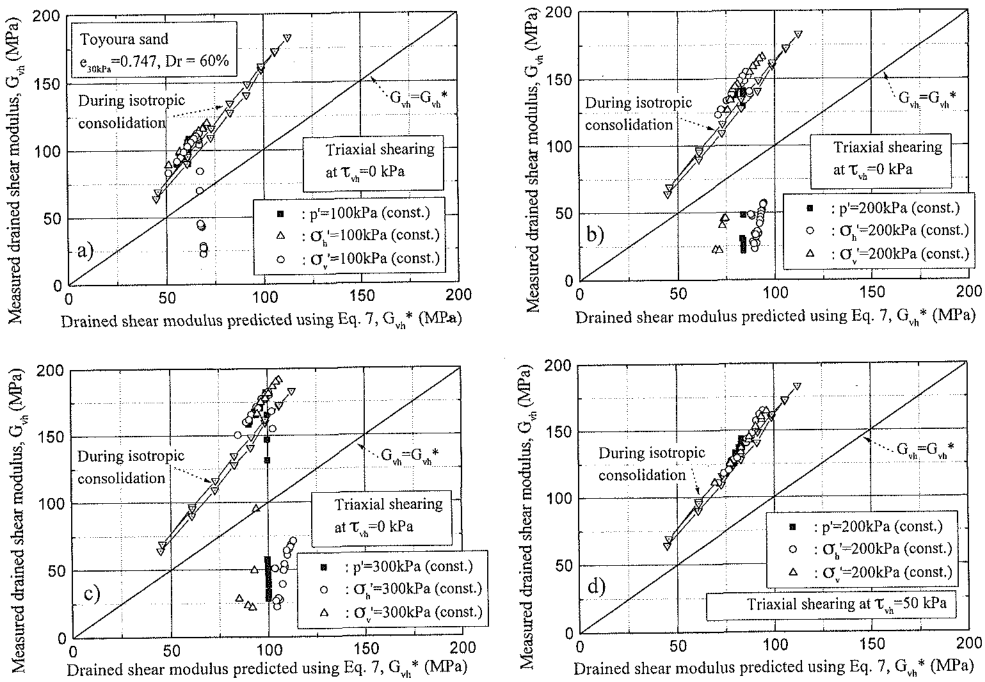

Figure 8. Comparison of drained quasi-elastic shear moduli that are predicted using Eq. 7 and measured during triaxial shearing starting from stress states with τ_{vh}=0 at a) $\sigma_v'=\sigma_h'$=100 kPa, b) $\sigma_v'=\sigma_h'$=200 kPa, c) $\sigma_v'=\sigma_h'$=300 kPa, and d) with τ_{vh}=50 kPa at $\sigma_v'=\sigma_h'$=200 kPa

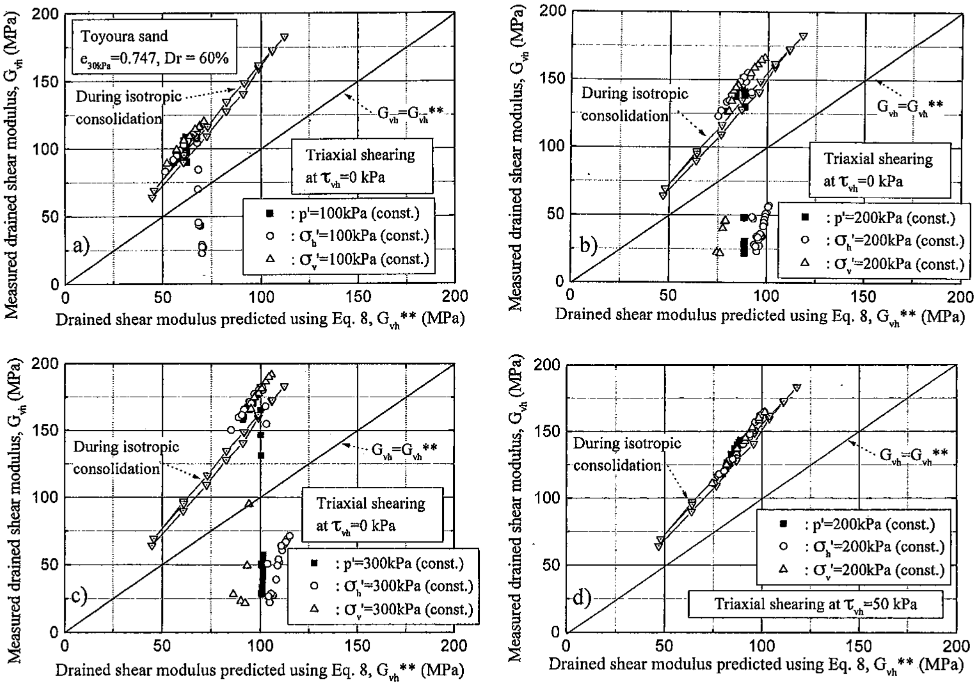

Figure 9. Comparison of drained quasi-elastic shear moduli that are predicted using Eq. 8 and measured during triaxial shearing starting from stress states with τ_{vh}=0 at a) σ_v'=σ_h'=100 kPa, b) σ_v'=σ_h'=200 kPa, c) σ_v'=σ_h'=300 kPa, and d) with τ_{vh}=50 kPa at σ_v'=σ_h'=200 kPa

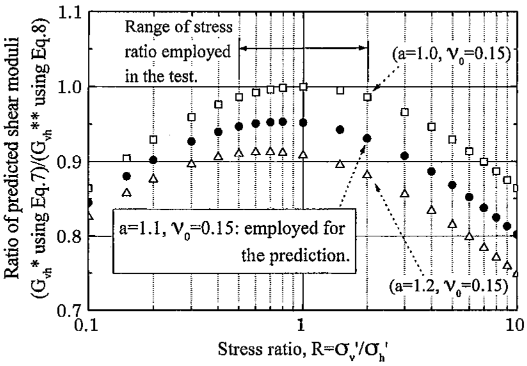

Figure 10. Ratio of predicted G_{vh} values using Eq. 7 to those using Eq. 8 versus stress ratio

predicted G_{vh} values using Eq. 7 to those using Eq. 8, which is eaual to $\{2(1-\nu_0)/(R^{-n/2}+aR^{n/2}-2a^{1/2}\nu_0)\}$, does not change largely from unity under the above range of R as shown in Fig. 10. Therefore, when the inherent anisotropy in the quasi-elastic Young's moduli is not large (i.e., when the a value is close to 1.0), Eq. 8 can be regarded as an approximation of Eq. 7.

CONCLUSIONS

The results from drained torsional and triaxial shear tests on Toyoura sand with externally measuring change of quasi-elastic deformation properties could be summarized as follows.

Under triaxial extension condition, the shear modulus that was defined on the vertical plane was found to be basically a function of $\sigma_m'=(\sigma_v'+\sigma_h')/2$ or $(\sigma_v'\sigma_h')^{0.5}$, where σ_v' and σ_h' are the vertical and horizontal stresses, respectively. The results could be also explained by a cross-anisotropic hypo-quasi-elastic model, considering inherent and stress state-induced anisotropy in modeling of vertical and horizontal Young's moduli and Poisson's ratios, as proposed by Tatsuoka et al. (1999).

Under triaxial compression condition, extensive degradation in the values of the shear modulus and the vertical Young's modulus was observed with the increase in the deviator stress $q=\sigma_v'-\sigma_h'$, and the extent of degradation was reduced by applying sustained shear stress on the vertical and horizontal planes. When the q value exceeded about 100 kPa, the quasi-elastic deformation properties started to recover with increase in the q value. It was estimated that these peculiar behaviors are affected by non-uniform distribution of vertical and torsional shear stresses applied to the specimen, on which further investigations are required.

REFERENCES

Ampadu, S.K. and Tatsuoka, F. (1993): "Effect of setting method on the behaviour of clays in triaxial compression from saturation to undrained shear," Soils and Foundations, Vol.33, No.2, pp.14-34.

Hardin,B.O. and Richart,F.E. (1963): "Elastic wave velocities in granular soils," *J. Soil Mech. Found. Div.*, ASCE, Vol.89, No.1, pp.33-65.

Hardin,B.O. and Bladford,G.E. (1989): "Elasticity of articulate materials," *J. Geotechnical Engineering*, ASCE, Vol.115, No.6, pp.788-805.

Hoque E. and Tatsuoka, F. (1998): "Anisotropy in elastic deformation of granular materials," *Soils and Foundations*, Vol. 38, No. 1, pp.163-179.

Jamiolkowski, M., Lancellotta, R. and Lo Presti, D.C.F. (1995): "Remarks on the stiffness at small strains of six Italian clays," *Pre-failure Deformation of Geomaterials*, Shibuya, Mitachi and Miura (eds.), Balkema, Vol. 2, pp. 817-836.

Koseki, J., Kawakami, S., Nagayama, H. and Sato, T. (2000): "Change of small strain quasi-elastic eeformation properties during undrained cyclic torsional shear and triaxial tests of Toyoura sand," accepted for publication in *Soils and Foundations*.

Tatsuoka, F., Kato, H., Kimura, M. and Pradhan, T.B.S. (1988): "Liquefaction strength of sands subjected to sustained pressure," *Soils and Foundations*, Vol. 28, No. 1, pp.119-131.

Tatsuoka, F. and Kohata, Y. (1995): "Stiffness of hard soils and soft rocks in engineering applications," *Pre-failure Deformation of Geomaterials*, Shibuya, Mitachi and Miura (eds.), Balkema, Vol. 2, pp. 947-1043.

Tatsuoka, F., Ishihara, M., Uchimura, T. and Gomes Correia, A. (1999): "Non-linear resilient behaviour of unbound granular materials predicted by the cross-anisotropic hypo-quasi-elasiticity model," *Unbound Glanular Materials*, Gomes Correia (ed.), Balkema, pp. 197-204.

Yamashita, S. and Suzuki, T. (1999): "Young's and shear moduli under different principal stress directions of sand," *Pre-failure Deformation Characteristics of Geomaterials*, Jamilokowski, Lancellotta and Lo Presti (eds.), Balkema, Vol.1, pp.149-158.